



Cationic Surfactant-Induced Instantaneous Gelation of Silk Fibroin Solution†

SHENZHOU LU^{1,*}, SHAN SUN², FANG ZHANG², JIAOJIAO LI², TIELING XING² and JIAN JIN^{1,*}

¹National Engineering Laboratory for Modern Silk, College of Textile and Clothing Engineering, Soochow University, Suzhou, P.R. China

²Suzhou Institute of Nano-Tech and Nano-Bionics, Chinese Academy of Sciences, Suzhou, P.R. China

*Corresponding author: E-mail: jjin2009@sinano.ac.cn

AJC-15769

Modern traumatic wound-care products have several associated disadvantages. They do not meet requirements because they lack good permeability, biocompatibility and air tightness. In an attempt to overcome these shortcomings, a new type of flexible, instantaneously-formed hydrogels resulting from blending silk fibroin and cationic surfactants with different carbon chains are introduced in this work. The secondary structure of these hydrogels is similar to that of a silk fibroin solution as they primarily consist of random coils. However, the structure is different from a pure silk fibroin hydrogel which primarily consists of β -sheet structure. By means of SEM, silk fibroin molecules form clustered nanofilaments during the cationic surfactant-induced hydrogelation, which is different from a pure silk fibroin hydrogel that is composed of a porous network structure. The charge effect, hydrophobic effect and surface tension are presumed to be related to the formation of the cationic surfactant/silk fibroin hydrogels.

Keywords: Natural materials, Silk fibroin, Hydrogel, Cationic surfactant.

INTRODUCTION

Hydrogels are chemically or physically cross-linked, three-dimensional polymer networks that are durable enough to swell in aqueous solutions, yet they do not dissolve in these solutions¹. Nowadays, various kinds of both synthetic and natural hydrogel materials have been developed to form hydrogels². Due to these materials' potential advantages, hydrogels have been comprehensively investigated in many aspects, such as their physical and chemical properties, biocompatibility and formation mechanism.

Silk fibroin (SF) is a biosynthesized fibrous protein that is extracted from the domesticated silkworm's cocoons (*Bombyx mori*). Because the material has outstanding biocompatibility, biodegradability by enzymatic or oxidative processes³ and a hydrophilic nature, silk fibroin-based hydrogels have extensive potential for biomedical application, including scaffolds for soft tissue engineering, drug delivery systems, encapsulation materials for gene or cell therapeutics, wound dressings, *etc.*^{4,5}. The hydrogelation of silk fibroin is triggered by altering either physical or chemical conditions, such as the pH, temperature, or additives⁶. Hydrogelation can also be triggered by changing the solution condition *via* ultrasonication or vortexing as energy inputs⁷. However, the clinical appli-

cation of silk fibroin is limited because of its time consuming nature; it often takes too long to form a hydrogel unless non-physiological treatments are used (*e.g.*, low pH and high temperature)⁸. In an attempt to combat this disadvantage, some studies have reportedly added polyethylene oxide (PEO) and polymeric surfactants to accelerate the hydrogelation, but they only shortened the hydrogelation time for a limited range⁹. Furthermore, Wu *et al.*¹⁰ found that adding sodium dodecyl sulphate (SDS) as the gelling agent under mild conditions (37 °C and pH 7.0 \pm 0.2) could reduce the silk fibroin gelation time. A special proportion of silk fibroin and SDS can induce rapid gelation based upon hydrophobic interactions and electrostatic effects. However, the fastest hydrogelation process still needs 15 min. Thus, finding an ideal additive that can form an instantaneous silk fibroin hydrogel with good mechanical properties is a priority in hydrogel development.

In this work, a cationic surfactant, functioning as a gel accelerator, was mixed into a silk fibroin solution at 37 °C. As soon as the solution was blended, it immediately formed a hydrogel. Furthermore, the instantaneously formed hydrogels had good elasticity. Therefore, these instantaneously formed silk fibroin hydrogels have the potential to contribute greatly to developments in wound dressings and drug delivery.

†Presented at 2014 Global Conference on Polymer and Composite Materials (PCM2014) held on 27-29 May 2014, Ningbo, P.R. China

EXPERIMENTAL

The following materials were purchased from Sigma-Aldrich (St. Louis, MO): Cationic surfactants (CSs) consisting of different carbon chain lengths, decyl trimethyl ammonium bromide (DETAB), dodecyl trimethyl ammonium bromide (DTAB), cetyl trimethyl ammonium bromide (CTAB) and stearyl trimethyl ammonium bromide (STAB).

Preparation of silk fibroin solution: Raw silk fibers from *B. mori* were degummed three times in a 0.05 % (w/w) sodium bicarbonate solution at 98–100 °C for 0.5 h and were then rinsed thoroughly with deionized water in order to remove glue-like sericin proteins. After drying at 60 °C, the extracted silk was then dissolved in a 9.3 M LiBr solution at 65 °C for 1 h. This was followed by dialysis with cellulose tubular membranes (molecular weight cut-off, 8,000–14,000) against distilled water for 3 days. The silk fibroin concentration was determined by weighing the remaining solid of a known volume of silk solution that had been dried at 105 °C. In order to keep the silk fibroin solution fresh for a long time, the silk fibroin solution was autoclaved for 10 min at 110 °C¹¹. A lower concentration silk solution was prepared by diluting the 60 g/L (w/v) stock solution with deionized water¹².

Gelation time of silk hydrogel: The purified silk solution was mixed with differing concentrations of DETAB, DTAB, CTAB and STAB. Because the silk fibroin solution starts to gel as soon as the cationic surfactant solution is added into the solution, the water and cationic surfactant solution were pipetted in first and then the silk fibroin solution was gently pipetted into each well of 24-well plates (Greiner Bio-one, Germany). The volume of the mixed solution was approximately 500 μ L. The plates were incubated in a Synergy HT Multi-Mode Microplate Reader (Bio-Tek Instruments, USA) at 37 °C. To monitor the gelation process as well as determine the gelation time, the turbidity changes occurring during gelation were measured using the instrument's absorbance mode (550 nm) at defined intervals. The turbidity change was defined by the optical density change (OD). For each concentration, six samples were measured and the values were averaged in order to determine the time course of optical density changes³. The optical density did not change immediately as the gelation of the mixed solution is a process; therefore, the time at which the optical density begins to change was regarded as the starting time of hydrogel formation. Accordingly, the end time was designated as the time point at which the optical density ceased changing.

The cross-section morphology was prepared by cutting the freeze-dried hydrogels with a razor blade. Next, the cross sections were coated with platinum for 90 s and then observed morphologically by SEM (S-4800, Hitachi, Tokyo, Japan). The various hydrogels' structures were analyzed by FTIR using a Magna spectrometer (Nicolet 5700) in the spectral region of 4000–400 cm^{-1} . The freeze-dried hydrogels were ground into a powder and then pressed into potassium bromide (KBr) pellets before data collection. Crystal structure was determined by X-ray diffraction (XRD). The experiments were conducted with an X-ray diffractometer (X2 Pert-Pro MPD, PANalytical, Almelo, Holland) at a 40 kV tube voltage and a 40 mA tube current. $\text{CuK}\alpha$ radiation was used with a diffraction angle of $2\theta = 5\text{--}45^\circ$ and the scanning rate was $2^\circ/\text{min}$ for the freeze-dried powdered gels.

Surface tension (SFT, γ) measurements of the silk fibroin solution and aqueous solutions of cationic surfactant with different concentrations were carried out using the Wilhemy plate method¹⁰ on a digital DataPhysics Tensiometer (Model: DCAT21, Germany) at 37 °C. The temperature was controlled by an F12-ED refrigerated/heating circulator bath (Julabo, Germany) using water for circulation. The lift motor speed used for detecting the solution surface was 1.00 mm/s. The test was stopped when the standard deviation of the surface tension was less than 0.03 mN/m over the last 50 measurement cycles. The accuracy was 0.001 mN/m. The determined surface tension data of the above solutions was plotted as a function of concentration to obtain the minimum cationic surfactant concentration with the lowest surface tension at the air/water interface.

Mechanical properties: The specimens' compression properties ($d = 14$ mm, $h = 9$ mm) were determined using an Instron-3366 testing frame (Instron, Norwood, MA) with a 10 N capacity load cell. After balancing at 37 °C for 2 h, the hydrogels' mechanical properties were measured at 25 °C with a cross head speed of 2 mm min^{-1} . All samples were measured in triplicate and then averaged.

Rheological measurements: An AR2000 rheometer was used for rheological measurements. Each sample was loaded into the rheometer with emphasis on not shearing or stretching the sample. A low strain of 1 % was chosen to make a frequency sweep from 1–100 rads and G' , G'' and $\tan \delta$ data were collected. The plate diameter is 20 mm and the angle of the cone is 1° .

RESULTS AND DISCUSSION

Gelation time of silk fibroin/cationic surfactant (SF/CS) solution: Cationic surfactants with different carbon chains were mixed into a silk solution at different concentrations and the final silk fibroin concentration in the mixed solution was 50 g/L. The gelation time was determined at 37 °C based upon time-dependent optical density values. The relationship between the varying optical density of the native silk solution and the SF/CS mixtures over time is shown in Fig. 1(a–e). The relationship between the gelation time and the cationic surfactants concentration is displayed in Table-1. The initial time is the point at which gelation began, whereas the latter one is the point at which gelation was finished. A start time of zero means gel formation began instantly. As the cationic surfactant concentration was increased, the mixture solutions began gelation earlier and a shorter time was needed for completing the gelation process. Additionally, longer alkyl chain length was also determined to quicken the gelation process; as the alkyl chains became longer (up to 16) the gelation process started earlier and needed less time for completion. Nevertheless, STAB had a limited solubility (up to 20 mM) in silk fibroin due to its overlong carbon chain.

Structural analysis: Fig. 2(A) and (B) show the XRD and FTIR of the freeze-dried samples derived from SF/CS hydrogels, pure silk fibroin hydrogel and silk fibroin solution (SFS). X-ray diffraction was performed in order to study the hydrogels' crystalline structure changes. The silk fibroin hydrogel produced diffraction peaks at about 9.1° , 20.4° and 24.3° , whereas the SF/CS hydrogels only produced a diffraction

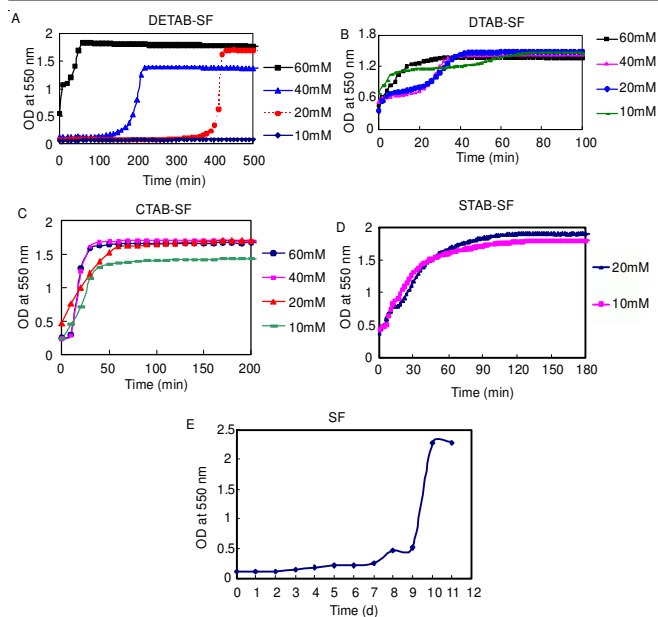


Fig. 1. Gelation process of cationic surfactant/silk fibroin solution under 37°C. SF-DETAB and SF-CTAB: measured every 10 min. SF-DTAB and SF-STAB: measured every 2 min. silk fibroin: measured every 24 h. The silk fibroin concentration in the mixed solution was 50 g/L

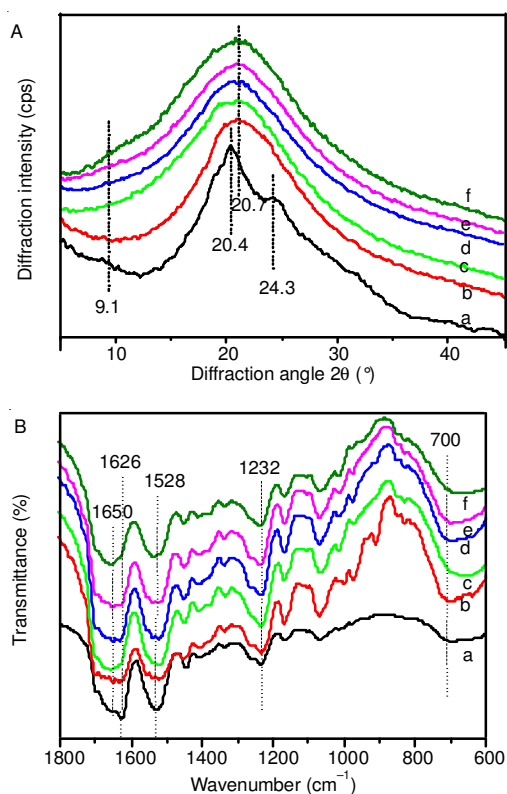


Fig. 2. XRD curves (A) and FTIR (B) obtained from a freeze-dried gel prepared under 37°C. (a) pure silk gel, (b) SF/DETAB with 60 mM DETAB (c) SF/DTAB with 10 mM DTAB, (d) SF/CTAB with 20 mM CTAB, (e) SF/STAB with 20 mM STAB, (f) silk solution. The silk fibroin concentration in the mixed solution was 50 g/L

peak at 20.7° and did not exhibit any distinct diffraction peaks at 9.2° and 24.3° , similar to that of the silk fibroin solution. They all showed an amorphous state, characterized by the presence of a broad peak in the scattering angle range of $10\text{--}30^\circ$ ¹³. This result indicates that the same crystalline structure

resulted from the cationic surfactants-induced instantaneous silk fibroin hydrogels and from the silk fibroin solution. The SF/CS hydrogels will keep their excellent elastic properties with non-crystalline structures.

The infrared (IR) spectral region within $1700\text{--}1500\text{ cm}^{-1}$ is assigned to absorption by the peptide backbones of amide I ($1700\text{--}1600\text{ cm}^{-1}$) and amide II ($1600\text{--}1500\text{ cm}^{-1}$), which have been commonly used for the analysis of different secondary structures of silk fibroin. The peaks at $1630\text{--}1610\text{ cm}^{-1}$ (amide I) and $1530\text{--}1520\text{ cm}^{-1}$ (amide II) are characteristic of the β -sheet structure, whereas the peaks at $1650\text{--}1630$ and $1545\text{--}1535\text{ cm}^{-1}$ are indicative of random coil structures¹⁴. The amide I and II bands for the pure silk fibroin hydrogel showed strong peaks at 1626 and 1528 cm^{-1} , corresponding to the β -sheet structure. As for the specimen prepared from the SF/CS hydrogels, absorptions at 1650 cm^{-1} appeared, which indicates that more random structures were maintained in the SF/CS hydrogels, similar to the silk fibroin solution. In other words, the gelation process is accompanied by a transition of the silk fibroin conformation from a primarily random coil structure in the solution to a principally β -sheet structure in the gel, whereas the silk fibroin conformation only minimally changed as the cationic surfactants were added. The SF/CS hydrogels still kept the random coil structure but did not change to the β -sheet structure.

Morphology: The hydrogels' morphological features were observed by SEM after being lyophilized. As shown in Fig. 3(A), the hydrogel resulting from the pure silk fibroin solution formed a porous network structure in which the pore diameters ranged from $2\text{--}5\text{ }\mu\text{m}$. The cationic surfactant-induced silk fibroin hydrogels, on the other hand, displayed synaptic-like structures with plenty of random coils that were highly cross-linked [Fig. 3(C-E)], which was in accordance with the silk fibroin solution [Fig. 3(B)]. This indicates that blending the cationic surfactant could induce the self-assembly of silk fibroin to nanofilament, which would further restrain the formation of lamellar structures during the hydrogelation process. Moreover, a number of micro globular structures were seen in the SEM images of the cationic surfactant-induced silk fibroin hydrogels, demonstrating that a great deal of water was stored in the hydrogels. This structure would generate excellent elastic properties in the cationic surfactant-induced hydrogels. From structural analysis, it is revealed that the cationic surfactant would restrain the secondary structure transition of silk fibroin from non-crystalline structures (random coil, α -helix) to crystal structures (Silk I and Silk II)¹⁵.

Rheological properties: The transition of sol-to-gel is primarily expressed by changes in the viscoelasticity. Therefore, viscoelasticity is a crucial index for determining the value of the gel fracture system. The hydrogels were measured as soon as the cationic surfactants were blended into the silk fibroin solution. The angular frequency dependence of the storage (G') and the loss modulus (G'') are shown in Fig. 4. For all of the hydrogels, as the angular frequency increased, both G' and G'' raised. However, the raised increment of G' was much more than that of G'' . Moreover, G' was greater than G'' throughout the entire process. This demonstrated that the elasticity was predominate in the mixture, particularly as

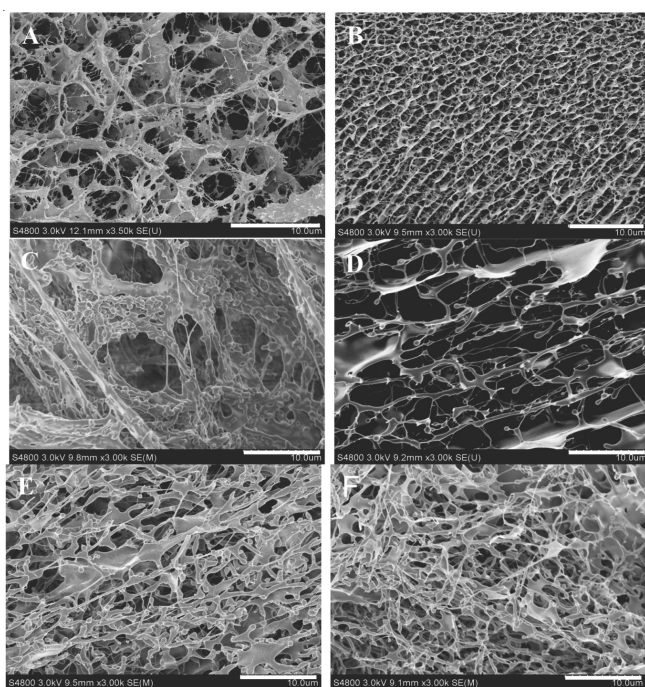


Fig. 3. SEM images (Scale Bar: 10 μm) for freeze-dried silk hydrogels prepared under 37 $^{\circ}\text{C}$. (A) pure silk gel, (B) DETAB/SFG with 60mM DETAB (C) DTAB/SFG with 10 mM DTAB, (D) CTAB/SFG with 20 mM CTAB, (E) STAB/SFG with 20 mM STAB, (F) silk solution. The silk fibroin concentration in the mixed solution was 50 g/L

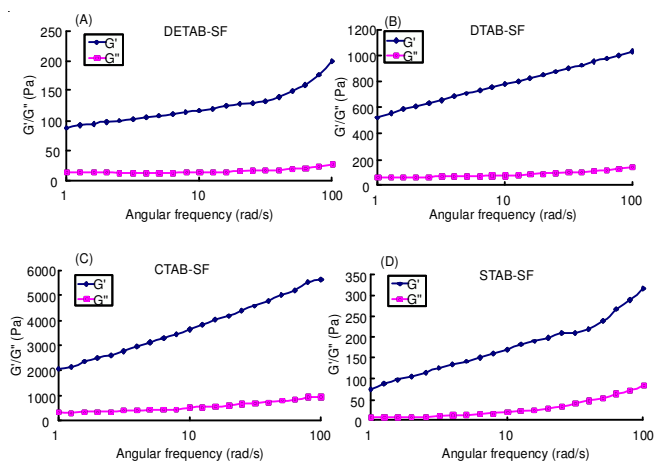


Fig. 4. Rheological property of SF-CS hydrogels measured under 37 $^{\circ}\text{C}$. DETAB/SFG: prepared with 60 mM DETAB. DTAB/SFG: prepared with 10 mM DTAB. CTAB/SFG: prepared with 20 mM CTAB. STAB/SFG: prepared with 20 mM STAB. The silk fibroin concentration in the mixed solution was 50 g/L

it reflected a typical hydrogel structure as soon as the cationic surfactants were blended. As the alkyl chain was extended, both G' and G'' grew, except for STAB. G' revealed high gel strength, so the gel could mold well and release the drug slowly. As for STAB, it could be interpreted with a necessarily longer gelation process. The phase angle indicates the correlation of elasticity and viscosity. The smaller that $\tan \delta$ is, the better the elasticity. $\tan \delta$ changes as related to angular frequency are shown in Fig. 5. For all four samples, $\tan \delta$ was less than 0.3 and changed only a little, which demonstrates an excellent elasticity¹⁶.

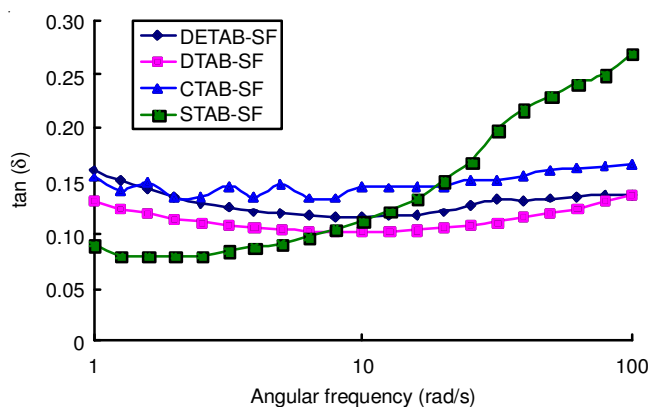


Fig. 5. $\tan \delta$ changes relating to angular frequency of SF-CS hydrogels

Mechanical properties: As shown in Fig. 6, all the comprehensive strain-stress curves exhibited a nonlinear behaviour, indicating that the samples possessed viscoelasticity. When the stress reached 35 %, the pure silk fibroin hydrogel began to fluctuate and a crack appeared in the hydrogel's interior. However, the stress of the cationic surfactant-induced hydrogel continued to increase up to a stress of 66 %. This reveals that the addition of cationic surfactant could enhance the failure strain of the silk fibroin hydrogel. The XRD results indicated that the cationic surfactants-induced, instantaneous silk fibroin hydrogels' structure was primarily of an amorphous state, which is the same crystalline structure as the silk fibroin solution. However, the XRD result for the pure silk fibroin hydrogel indicated that it largely consisted of β -sheet structure (silk II crystalline structure). With a high crystalline structure, the modulus of compressibility of the pure silk fibroin hydrogel was much higher than for the SF/CS hydrogels, which can be seen from Fig. 5. The pure silk fibroin hydrogel began to fluctuate and crack when the stress reached 35 %, which was also due to the β -sheet structure.

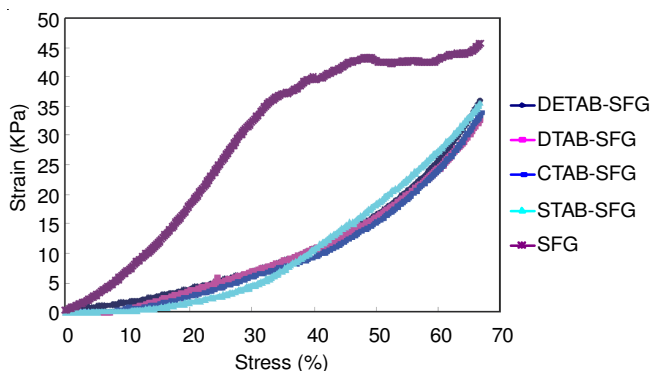


Fig. 6. Compressive stress-strain curves of silk hydrogels prepared under 37 $^{\circ}\text{C}$ for 2 h. DETAB/SFG: prepared with 60 mM DETAB. DTAB/SFG: prepared with 10 mM DTAB. CTAB/SFG: prepared with 20 mM CTAB. STAB/SFG: prepared with 20 mM STAB. The silk fibroin concentration in the mixed solution was 50 g/L

Surface tension of solutions: Surface tensiometry is a common and effective means of studying the interactions between proteins and surfactants. The relationship between surface tension (γ) and the cationic surfactant aqueous solution concentration is shown in Fig. 7. The native silk solution (50 g/L) showed a weak surface activity because of a lower surface

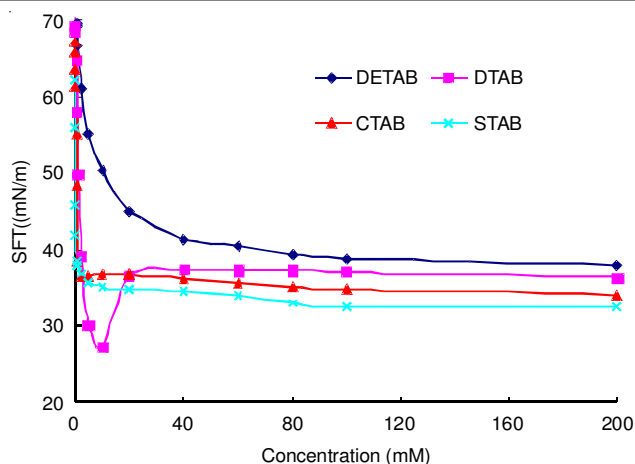


Fig. 7. Static surface tension of cationic surfactants in aqueous solution with different concentrations measured under 37 °C

tension (about 43 mN m⁻¹) as compared to pure water (72 mN m⁻¹). At first, with a lower than concentration, the surface tension dropped sharply; then, even as an increasing concentration was added, the surface tension still only experienced minimal change. Of particular interest is the surface tension of DTAB; it reached its minimum at more quickly than the others did. Next, it increased to 37 mN m⁻¹ before it finally remained relatively constant. This result indicated that cationic surfactants are obviously capable of decreasing the surface tension in an aqueous solution because they have both hydrophobic alkyl groups and hydrophilic amino groups. When a certain concentration is reached, the non-polar parts can combine with one another and distribute around the outside, which spatially encapsulates the hydrophilic group. As a result, micelles are formed.

As the carbon chain became longer, the surface tension was reduced. However, the surface tension of DTAB reached its minimum at 10 mM more quickly than the others. The concentration that can significantly reduce the surface tension of water was called the efficiency of the surfactant. The minimum surface tension was defined as the valid surfactant value. Clearly, the lower the surface tension dropped, the more effective the surfactant was. The efficiency and the valid value were usually opposite in value: *i.e.*, when the hydrophobic chain length was increased, the efficiency was improved and the valid value was lower. This relationship explains why DTAB is exceptional in comparison to both CTAB and STAB.

The surfactants were capable of reducing the surface tension of water and the interfacial tension between the oil and water. In comparing Fig. 7 with Table-1, the results show that once the surface tension is below 40 mN m⁻¹ (nearby the CMC of the cationic surfactants), the corresponding cationic surfactants concentration could stimulate the silk fibroin to form hydrogels instantaneously.

As is well-known, the gelation of silk fibroin is accompanied by a structural transition in the solution from random coil to β -sheets. The β -sheets then assemble to form a physically cross-linked gel network with conglomerate micron-sized protein-rich particles^{3,4,6,8}. In contrast, cationic surfactant-induced silk fibroin hydrogels primarily consist of random coils and the silk fibroin molecules form nanofilament that clusters during the hydrogelation. A thorough examination was conducted in order to determine the relevant characteristics of the formation of these hydrogels as well as how they interacted. According to a study on the effect that the quaternary ammonium salt cationic surfactant with different carbon chains has on the silk fibroin gelatinization, it appeared that the hydrogel formation was directly connected with the charge effect, the length of the hydrophobic carbon chains (hydrophobic effect) and the surface tension.

The fibroin molecule has an overall negative charge in neutral pH because it has an isoelectric point at pH = 4.1⁸; conversely, a cationic surfactant is positively charged because of its amino group. The strong electrostatic effect can lead to a rapid combination between the fibroin molecules and the cationic surfactant. At the same time, the charge tends to be neutral in the hybrid system and thus, the system becomes instable and the silk fibroin molecules aggregate together easily. This also generates a prime condition for fast association between the fibroid silk fibroin molecular chains. Nevertheless, adding some positive ions, such as a calcium ion, zinc ion or copper ion, into the silk fibroin solution would not instantaneously accelerate gelation. Therefore, the charge effect is not the only interaction in hydrogel formation.

In addition, only when the carbon chain length is equal to or greater than 8 can the cationic surfactant accelerate the gelation process. As the hydrophobic alkyl chain grew longer, the hydrophobic interactions between the silk fibroin molecules enhanced, thus leading to the self-assembly of the silk fibroin and, subsequently, a quicker hydrogel formation. However, too long of an alkyl chain will increase the steric hindrance between the silk fibroin molecule chains and alkyl chains, thus inhibiting the gelation.

Last but not least, as surfactants, DETAB, DTAB, CTAB and STAB had low surface tension near the CMC. They can decrease the interfacial tension between the silk fibroin molecules and function as a "lubricant." This is advantageous for the cationic surfactant-silk fibroin system to form a gel. In CMC, the cationic surfactant molecules were abundant enough to spread uniformly throughout the silk fibroin solution and come into contact with numerous silk fibroin molecules. Thus, the non-polar parts could combine with each other and consequently, the hydrophilic groups were packed outside the micelle. In this way, the low surface tension and the large number of cationic surfactant molecules worked together to

TABLE-1
GELATION TIME OF THE SILK FIBROIN/ CATIONIC SURFACTANT SOLUTION

Concentration (mM)	60	40	20	10	0
SF-DETAB	0→1 h	2.5→3.5 h	6→7 h	2d	
SF-DTAB	0→0.5 h	0→0.6 h	0→1 h	0→1 h	
SF-CTAB	0→0.5 h	0→0.5 h	0→1 h	0→1.5 h	10d
SF-STAB	—	—	0→2 h	0→2 h	

convert the silk fibroin molecules' interactions with each other into clustered nanofilaments.

In conclusion, the rapid formation of cationic surfactant-induced silk fibroin hydrogels results from the combination of several factors: the charge effect, hydrophobic effect and surface tension.

Conclusion

A method was developed to accelerate the self-assembly process of an silk fibroin solution into a nanofilament hydrogel by adding cationic surfactants with different carbon chains. The silk fibroin solution instantaneously formed into a hydrogel as soon as the cationic surfactants were mixed. These hydrogel's secondary structure was similar to that of the silk fibroin solution as the structure primarily consisted of random coils. The SF-CS hydrogels possessed good mechanical properties with good elasticity.

ACKNOWLEDGEMENTS

This work was supported by National Natural Science Foundation of China (Grant No. 51203107, 51373114), PAPD and Nature Science Foundation of Jiangsu, China (Grant No. BK20131176).

REFERENCES

1. C.C. Lin and A.T. Metters, *Adv. Drug Deliv. Rev.*, **58**, 1379 (2006).
2. X.Q. Wang, J.A. Kluge, G.G. Leisk and D.L. Kaplan, *Biomaterials*, **29**, 1054 (2008).
3. A. Matsumoto, J. Chen, A.L. Collette, U.-J. Kim, G.H. Altman, P. Cebe and D.L. Kaplan, *J. Phys. Chem. B*, **110**, 21630 (2006).
4. K. Numata, T. Katashima and T. Sakai, *Biomacromolecules*, **12**, 2137 (2011).
5. B. Balakrishnan and R. Banerjee, *Chem. Rev.*, **111**, 4453 (2011).
6. U.J. Kim, J. Park, C. Li, H.-J. Jin, R. Valluzzi and D.L. Kaplan, *Biomacromolecules*, **5**, 786 (2004).
7. T. Yucel, P. Cebe and D.L. Kaplan, *Biophys. J.*, **97**, 2044 (2009).
8. S. Nagarkar, T. Nicolai, C. Chassenieux and A. Lele, *Phys. Chem. Chem. Phys.*, **12**, 3834 (2010).
9. T.Y. Zhong, Z.G. Xie, C.M. Deng, M. Chen, Y. Gao and B. Zuo, *J. Appl. Polym. Sci.*, **127**, 2019 (2013).
10. X.L. Wu, J. Hou, M.Z. Li, J. Wang, D.L. Kaplan and S. Lu, *Acta Biomater.*, **8**, 2185 (2012).
11. X.L. Wu, L. Mao, D.K. Qin and S.Z. Lu, *Adv. Mater. Res.*, **311-313**, 1755 (2011).
12. N. Guziewicz, A. Best, B. Perez-Ramirez and D.L. Kaplan, *Biomaterials*, **32**, 2642 (2011).
13. Q. Lu, X. Hu, X. Wang, J.A. Kluge, S. Lu, P. Cebe and D.L. Kaplan, *Acta Biomater.*, **6**, 1380 (2010).
14. X. Chen, D.P. Knight, Z.Z. Shao and F. Vollrath, *Polymer (Guildf.)*, **42**, 9969 (2001).
15. S.Z. Lu, X.Q. Wang, Q. Lu, X. Zhang, J.A. Kluge, N. Uppal, F. Omenetto and D.L. Kaplan, *Biomacromolecules*, **11**, 143 (2010).
16. A.E. Terry, D.P. Knight, D. Porter and F. Vollrath, *Biomacromolecules*, **5**, 768 (2004).